Conical antiferromagnetic order in the ferroelectric phase of Mn$_{0.8}$Co$_{0.2}$WO$_4$ resulting from the competition between collinear and cycloidal structures

I. Urcelay-Olabarria[*]

Institut Laue Langevin, 6 rue Jules Horowitz BP 156, F-38042 Grenoble cedex 9, France

E. Ressouche

SPSMS, UMR-E CEA/UJF-Grenoble 1, INAC, F-38054 Grenoble, France

A. A. Mukhin and V. Yu. Ivanov

Prokhorov General Physics Institute, Russian Academy of Science, Vavilov St., 38, 119991 Moscow, Russian Federation

A. M. Balbashov

Moscow Power Engineering Institute, 105835 Moscow, Russia

J. L. García-Muñoz

Institut de Ciència de Materials de Barcelona, ICMAB-CSIC, Campus Universitari de Bellaterra, E-08193 Bellaterra, Spain

V. Skumryev

Institució Catalana de Recerça i Estudis Avancats, E-08010 Barcelona, Spain and
Departament de Física, Universitat Autònoma de Barcelona, E-08193 Bellaterra, Spain

Evolution of competing commensurate collinear (AF4) and incommensurate cycloidal (AF2) magnetic structures in Mn$_{0.8}$Co$_{0.2}$WO$_4$ multiferroic was studied by neutron diffraction, magnetic, and pyroelectric characterization measurements. In contrast to pure and slightly Co doped MnWO$_4$, the antiferromagnetic AF4 collinear phase [$\mathbf{k}_1 = (\frac{1}{2},0,0)$] inherent to the pure CoWO$_4$ was observed below Néel temperature $T_N \approx 20$ K in Mn$_{0.8}$Co$_{0.2}$WO$_4$. This collinear order survives down to the lowest temperature reached in the experiments (2 K) even after the appearance of the second (cycloidal AF2) spin order below $T_{FE} \approx 8.5$ K [$\mathbf{k}_2 = (-0.211,\frac{1}{2},0.452)$]. Ferroelectric polarization along b axis was revealed below T_{FE} in the low temperature conical phase resulting from the superposition of the AF4 and AF2 spin structures. The arrangement of the spins after the two successive magnetic transitions are thoroughly described. In particular, we found that spins in the AF4 phase are aligned along the easy direction in the ac plane ($\sim 142°$ with respect to the c^* axis), while the cycloidal AF2 spin order is developed in the magnetically hard directions, perpendicular to the easy one, and consequently the T_{FE} decreases compared to the pure MnWO$_4$.

PACS number(s): 75.85.+t, 75.25.−j, 75.50.Ee

I. INTRODUCTION

A significant interest in magnetoelectric multiferroic materials was stimulated in past years by the discovery of a new kind of multiferroics in which the ferroelectric ordering has an improper character and is induced by complex magnetic structures.[1–4] A common feature of such multiferroics is the competition of exchange interactions which often results in the formation of incommensurate noncollinear magnetic structures, in particular, those of a cycloidal type allowing a ferroelectric polarization due to the break of the spatial inversion symmetry. The inverse Dzyaloshinskii-Moriya mechanism favors canted magnetic moments and atomic displacements, which can generate electric polarization in the direction given by $\mathbf{P} \sim \mathbf{r}_{ij} \times (\mathbf{S}_i \times \mathbf{S}_j)$. Namely, this magnetoelectric coupling contributes to the polarization when the nonzero spin-chirality $(\mathbf{S}_i \times \mathbf{S}_j)$ is noncollinear with respect to the radial vector $\mathbf{r}_{ij}$ connecting neighboring $\mathbf{S}_i$ and $\mathbf{S}_j$ spins.[5–7]

MnWO$_4$ is one of the prototype compounds of these new multiferroics in which ferroelectricity is induced by a cycloidal spin structure.[8–12] Its crystal structure has the symmetry $P2/c$

(No. 13, b-unique axis, standard setting) and it undergoes successive magnetic transitions into three different antiferromagnetic phases: collinear sinusoidally ordered AF3 phase at $T_N = 13.5$ K with propagation vector $\mathbf{k} = (-0.221,\frac{1}{2},0.457)$ and spins along easy axis in the ac plane, then at 12.5 K the ferroelectric ($\mathbf{P} \parallel b$) spin cycloidal AF2 phase appears with the same propagation vector, and below 7.5 K it is transformed to the collinear paraelectric and commensurate AF1 phase with $\mathbf{k} = (\pm\frac{1}{4},\frac{1}{2},\frac{1}{2})$. The observed succession of the various magnetic structures and the phase transitions indicates a strong competition and subtle balance among multiple magnetic interactions[12] which can be modified by chemical doping.

The evolution of the multiferroic phases and ferroelectric properties in Mn$_{1-x}T_x$WO$_4$, where Mn^{2+} is substituted by T^{2+} ions (T = Fe, Co, Mg, Zn), has been the subject of numerous studies.[13–22] In particular, for the Co substituted system at cobalt concentrations above $\sim$ 3% the commensurate AF1 phase is suppressed and the ferroelectric cycloidal phase AF2 with $\mathbf{P} \parallel b$ remains stable down to the lowest temperatures. With further increasing of cobalt concentration, at $x = 0.1$, the spin cycloidal plane flops to the ac plane accompanied by

reorientation of the polarization to the same plane.[15,18,22] At higher doping ($x = 0.15$) a new antiferromagnetic AF4 phase with wave vector $\mathbf{k} = (\frac{1}{2}, 0, 0)$, inherent to the pure CoWO$_4$, arises below $T_N \approx 15$ K and competes with the cycloidal and collinear phases found in MnWO$_4$. This results in a complicated scenario of phase transitions between different spin structures.[19]

In this work we have investigated the magnetic and electric polarization properties of Mn$_{0.8}$Co$_{0.2}$WO$_4$ single crystals. The spin structures determined by neutron diffraction measurements confirm the relevance of the competition between the magnetic anisotropy and the isotropic exchange interactions.

II. EXPERIMENTS

Single crystals of Mn$_{0.8}$Co$_{0.2}$WO$_4$ were grown by a floating zone method using a light heating.[23] The crystal growth was performed in an air atmosphere at a linear speed 8–10 mm/h with a counter-rotation of crystal and feed rod $\sim$20 min^{-1}. Finally, the crystal was annealed at $T = 1100\,^\circ$C. Samples with dimensions suitable for the particular measurements and with different crystallographic orientations were cut from the same crystal.

Magnetization was measured as a function of temperature using a superconducting quantum interference device (SQUID) magnetometer from Quantum Design. A magnetic field of 1 kOe was applied within a few degrees of accuracy along distinctive magnetic directions and also along the principle crystallographic directions of the crystal (shaped as a $5 \times 1.5 \times 0.8$ mm^3 parallelepiped). The data presented here are not corrected for the demagnetizing field effect.

The neutron diffraction experiments were carried out on the CEA-CRG single crystal diffractometer D23 at the Institut Laue Langevin (Grenoble, France), using a wavelength $\lambda = 1.277$ Å. The crystal used in the bulk magnetic measurements was mounted inside a magnet and its crystallographic a axis was set vertical with respect to the laboratory frame of reference. All nuclear peaks accessible in this geometry (273 independent reflections) were collected in the paramagnetic state at 25 K. The magnetic peaks were collected at 11 K and 2 K and the temperature dependence of two of them was monitored from 2 K up to 25 K. The neutron absorption in the sample ($\mu = 0.041$ mm^{-1}) has been corrected using the Cambridge Crystallography Subroutine Library[24] and the structure refinements were done using the FULLPROF SUITE package.[25] Data treatments were done by least square refinements of the integrated intensities. The refinements included an extinction correction following the model of Becker-Coppens. For determining the magnetic structures, the nuclear crystallographic parameters and the scale factors were fixed to the values obtained in the nuclear refinements.

For a given magnetic propagation vector $\mathbf{k}$ (and the associated $-\mathbf{k}$), the magnetic structure has been described according to the following expression:

$$\mathbf{m}_{lj}(\mathbf{k}) = \mathrm{Re}(m)\hat{u}_j \cos[2\pi(\mathbf{k} \cdot \mathbf{R}_l + \varphi_j)]$$
$$+ \mathrm{Im}(m)\hat{v}_j \sin[2\pi(\mathbf{k} \cdot \mathbf{R}_l + \varphi_j)], \quad (1)$$

where $\mathbf{m}_{lj}$ is the magnetic moment of the atom j in the unit cell l, $\mathbf{R}_l$ is the vector joining the arbitrary origin to the origin of unit cell l, and φ_j is a magnetic phase.

Electric polarization was studied along a, b, and c axes by pyroelectric measurements using a Keithley 6517A electrometer. The samples were cut platelike of thickness 0.85–1.9 mm. Electrical contacts were attached by Ag paint on the two parallel biggest surfaces with areas of 13–20 mm^2 each. In order to ensure a single domain ferroelectric state a poling field E_p up to ± 3000 V/cm was first applied in the paraelectric state at temperatures 15–30 K, prior to cooling the sample down to 1.9 K. For E_p above ± 2000 V/cm the polarization saturates to similar values of opposite signs and its temperature dependence upon heating, measured under electrical field or in zero field, was practically the same. All this suggests a single domain ferroelectric state. The temperature dependence of polarization upon heating or cooling was measured in swiping temperature mode with a rate of about 1 K/min, resulting in a small hysteresis of less than 1 K.

III. RESULTS

A. Magnetic properties

Figure 1(a) presents the temperature variation of susceptibility along the b axis and along two distinctive directions within the ac plane, namely for a field applied at an angle α of about 143° in respect to the c axis (named α axis) and for a field perpendicular to it. For those two orientations it was found that the susceptibilities at about 20 K have the highest and the lowest values, respectively. This is confirmed by the angular dependencies of the susceptibility measured in magnetic field of 1 kOe rotating in the ac plane shown in Fig. 1(b). At 25 K, above T_N, the angular dependency of the magnetic susceptibility along the easy (α) and hard ($\alpha + 90°$) directions exhibits its maximum and minimum value, respectively, whereas below T_N the situation is inverted. The difference of the susceptibilities in Figs. 1(a) and 1(b) is due to the small contribution from the rotator. The susceptibility in any other direction in the crystal was found to be a superposition between the three orientations presented in Fig. 1(a). The peculiarity at 20.2(2) K, clearly visible in the susceptibility along all the directions, could be naturally attributed to the Néel temperature, T_N. Another susceptibility anomaly at 8.6(3) K, which is evident for the two orientations perpendicular to α axis, signals a change in the magnetic structure. Within the experimental resolution no unambiguous fingerprint of this transition was detected on the susceptibility along the α direction.

As seen from Fig. 1(b), the anisotropy observed at T_N persists in the paramagnetic region with all the three inverse susceptibilities becoming parallel straight lines at high enough temperatures where the Curie-Weiss law applies. This reflects in significant difference in the asymptotic paramagnetic temperatures, Θ_P, obtained for the three directions: $\Theta_P = -70(2)$ K along b axis, $\Theta_P = -48(2)$ K for the α orientation, and $\Theta_P = -83(2)$ K for the orientation perpendicular to α within the ac plane. Within the experimental error, the effective magnetic moment was found to be the same for all the orientations 5.78(5) μ_B, a value which is somewhat higher
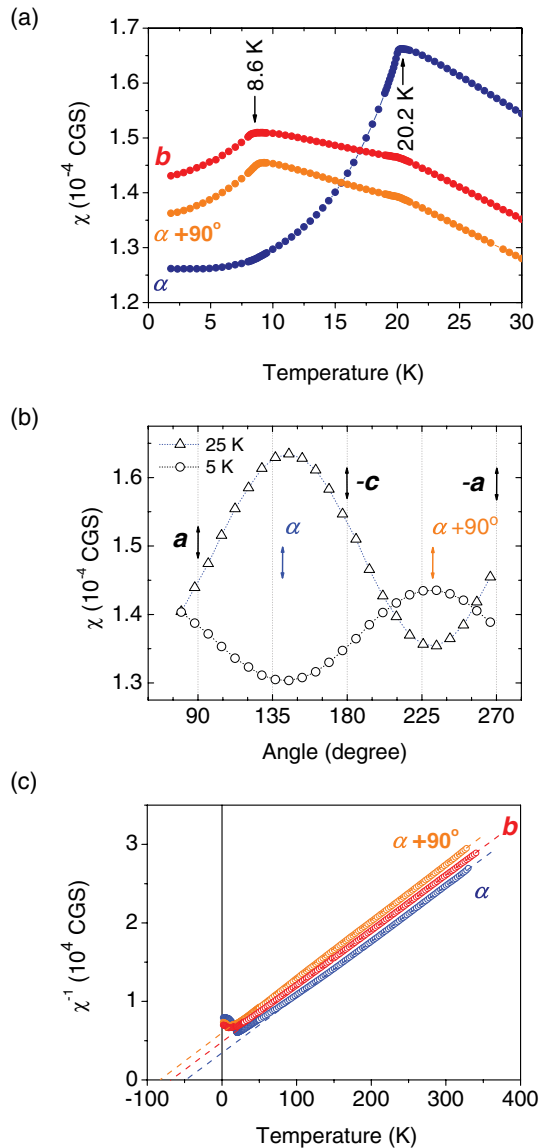
(a)

(b)

(c)

FIG. 1. (Color online) (a) Temperature dependence of suscepti-
bility along the b axis and along two distinctive directions within the
ac plane, namely for the field applied at an angle α of about 37° with
respect to the c axis and for the field perpendicular to it; (b) angular
dependencies of susceptibility in $H = 1$ kOe within the ac plane, at
25 and 5 K; (c) temperature dependence of the inverse susceptibility.

than the one expected from the Mn^{2+} ions and the spin only
contribution from the Co^{2+} ions (5.57 μ_B) and, thus, suggests
that the Co orbital moment is not completely frozen.

B. Neutron diffraction

The 20% cobalt doped compound is isostructural to pure
$MnWO_4$.[8] It crystallizes in the monoclinic $P2/c$ (No. 13,
standard setting) space group. The structure consists of chains
of oxygen-made octahedra along the c axis and the magnetic
atoms are located inside the octahedra; see Fig. 2(a). Cell
parameters obtained by centering 25 nuclear reflections at
25 K are the following: $a = 4.814(7)$ Å, $b = 5.731(2)$ Å,
$c = 4.976(2)$ Å, and $\beta = 90.70(7)°$. Table I gathers all the
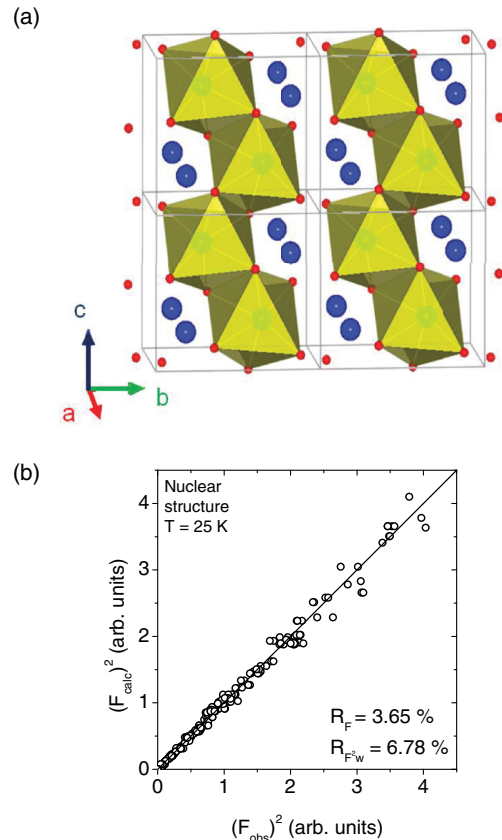refined parameters for the nuclear structure: atomic positions,

(a)

(b)

FIG. 2. (Color online) (a) Crystal structure of $Mn_{0.8}Co_{0.2}WO_4$.
Circles in the octahedra (green) correspond to Mn/Co, big (blue)
circles between the octahedra are tungsten atoms, and smallest circles
(red) are oxygen atoms. (b) Agreement plot of the nuclear structure
refinement at 25 K.

occupations, and atomic displacements parameters. The re-
fined amount of cobalt in the sample is 18.0(6)%, slightly
lower than the nominal value of 20%. Agreement plot of the
nuclear structure refinement is given in Fig. 2(b).

Below the Néel temperature, $T_N = 20$ K, two magnetically
ordered phases were found, one of which is characterized
by a single propagation vector $\mathbf{k}_1$, and the other one by
two vectors, $\mathbf{k}_1$ and $\mathbf{k}_2$. The centering of 20 reflections
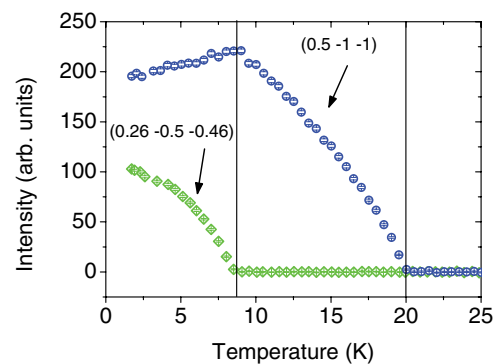at 2 K concluded that $\mathbf{k}_2 = [-0.211(1), \frac{1}{2}, 0.452(2)]$ is an

FIG. 3. (Color online) Integrated intensities of two magnetic
reflection as a function of the temperature. The error bars are inside
the symbols.

TABLE I. Crystal structure parameters of $Mn_{0.80}Co_{0.20}WO_4$, from refinement of 273 independent reflections collected. The space group is $P2/c$ and the atomic positions: Mn and Co at $2f$: $\frac{1}{2}$, y, $\frac{1}{4}$; W at $2e$: 0, y, $\frac{1}{4}$; and O at $4g$: x,y,z. Site occupancies and Debye-Waller factors ($Å^2$) are also included.

| Cell parameters: | | $a = 4.814(7)$ Å, $b = 5.731(2)$ Å, $c = 4.976(2)$ Å, $\beta = 90.70(7)°$ | | | |
Atoms	x	y	z	Occ.	B_{eq}
Mn		0.6847(5)		82.0(6)%	0.31(7)
Co		0.6847(5)		18.0(6)%	0.31(7)
W		0.1807(3)			0.08(3)
O1	0.2124(8)	0.1031(1)	0.9401(2)		0.24(2)
O2	0.2522(8)	0.3752(1)	0.3928(2)		0.24(2)
Rel. fac. $R_F = 3.65$, $R_{F^2} = 5.65$, $R_{F^2 w} = 6.78\%$					

incommensurate propagation vector, while on the contrary $\mathbf{k}_1 = (\frac{1}{2},0,0)$ is commensurate from T_N down to the lowest temperature. Figure 3 shows the evolution of two magnetic reflections characteristic of $\mathbf{k}_1$ and $\mathbf{k}_2$ with the temperature. When decreasing temperature, below 20 K the reflection related to $\mathbf{k}_1$ appears. Its intensity increases down to 8.5 K where there is a change in its evolution. At that point new reflections associated to $\mathbf{k}_2$ emerge. With further decreasing of temperature, the intensity of the latter reflection increases, whereas the intensity of the commensurate reflection slightly decreases.

Data collections were made in order to determine the magnetic structures at 2 K and 11 K. The parameters of the obtained magnetic structures are given in Table II, the spin arrangements are plotted in Figs. 4(a) and 4(b), and the agreement plots are depicted in Figs. 4(c) and 4(d). The magnetic structure at 11 K is a collinear one, the so-called AF4.[15,19] The moments lay in the ac plane, along the easy-axis α that makes an angle $\theta_u = 142(2)°$ with the c^* axis; see Fig. 4(a). In the collinear AF4 order the magnetic moments in the zigzag chains of octahedra running along the c axis are ferromagnetically coupled. Chains form ferromagnetic layers which extend parallel to the bc plane, and the adjacent layers along the a

axis are antiferromagnetically coupled. The ordered moment observed at 11 K is 3.17(7) μ_B per magnetic atom.

The same set of reflections related to $\mathbf{k}_1$ revealed no difference within the error bars in the magnetic component associated to $\mathbf{k}_1$ at 2 K. However, at that temperature there is an additional propagation vector and new magnetic reflections of the type $(hkl) \pm \mathbf{k}_2$ arise. The refinement of the 212 latter type of reflections allows us to conclude that the incommensurate part is an elliptical cycloid, the eccentricity of which is $\epsilon = 0.61$ according to the definition given in Ref. 22. The main axes of the cycloid are along b axis and a direction in the ac plane that makes and angle $\omega = 55(1)°$ with the c^* axis ($\omega = \alpha + 90°$). Therefore, the incommensurate part of the magnetic structure is rotating in a plane ($b\omega$) which is perpendicular to α (direction of the moments of the collinear component). The coexistence of two propagation vectors can thus be accounted for by a conical structure, as sketched in Fig. 4(b). Below T_{N2}, $\mathbf{m}_{conical} = \mathbf{m}_{AF2} + \mathbf{m}_{AF4}$ at each Mn/Co site. At 2 K the two components are rather similar: $m_{AF4} = 3.23\,\mu_B$ and $2.42\,\mu_B \leqslant m_{AF2} \leqslant 3.05\,\mu_B$ (since $\mathbf{m}_{AF2}$ is an elliptical helix). As a result, the maximum amplitude on the Mn/Co site is 4.44 μ_B. This value is practically the theoretical saturation moment expected for neutrons

TABLE II. Parameters that describe the magnetic structures of $Mn_{0.8}Co_{0.2}WO_4$. Magnetic atoms Mn_1 and Mn_2 are located in the crystallographic unit cell in [0.5, 0.6847(5), 0.25] and [0.5, 0.3153(5), 0.75], respectively. The unitary vectors, $\hat{u}$ and $\hat{v}$, are described by the spherical angles: ϕ is the angle that the projection of the moments in the ab plane makes with x ($\parallel a$) and θ the angle that the spins make with z ($\parallel c^*$). The weighted residual factors are $R_{F^2 w} = 9.11\%$, $R_{F^2 w} = 8.74\%$, and $R_{F^2 w} = 6.17\%$, respectively.

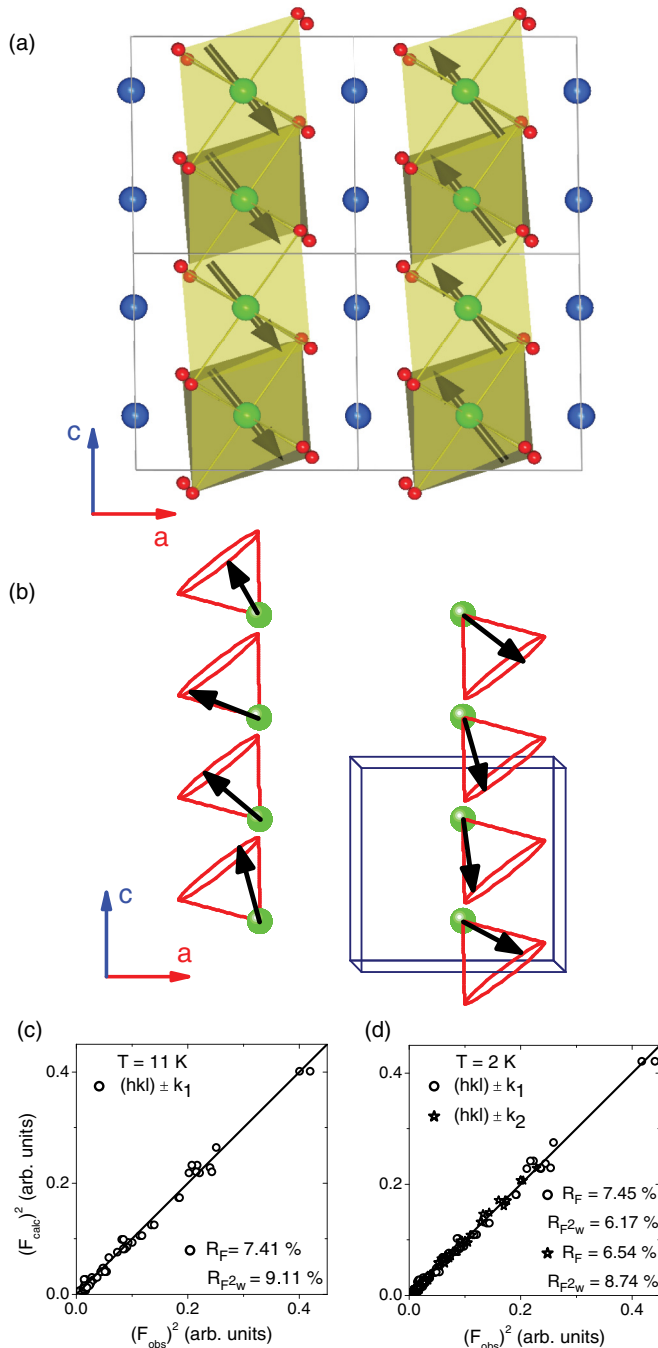|		$T = 11$ K	$T = 2$ K	$T = 2$ K
k		(0.5, 0, 0)	(0.5, 0, 0)	$[-0.211(1), 0.5, 0.452(2)]$
Mn_1				
	$Re(m)(\mu_B)$	3.15(2)	3.23(6)	3.05(3)
	ϕ_u	0	0	0°
	θ_u	142(2)°	143(2)°	55.0(9)°
	$Im(m)(\mu_B)$			$-2.42(4)$
	ϕ_v			90°
	θ_v			90°
Mn_2				
		$\mathbf{u}_2^{x,z} = \mathbf{u}_1^{x,z}$	$\mathbf{u}_2^{x,z} = \mathbf{u}_1^{x,z}$	$\mathbf{u}_2 = -\mathbf{u}_1$
		$\mathbf{u}_2^y = \mathbf{u}_1^y = \mathbf{v}_1 = \mathbf{v}_2 = 0$	$\mathbf{u}_2^y = \mathbf{u}_1^y = \mathbf{v} = 0$	$\mathbf{v}_2 = -\mathbf{v}_1$
$\Delta\varphi$		$0 = \frac{k_z}{2}$	$0 = \frac{k_z}{2}$	$0.226(1) = \frac{k_z}{2}$

FIG. 5. (Color online) Temperature dependence of electric polarization along b axis in $E = 0$. Data was collected while heating, after cooling the sample from the paraelectric state down to 1.9 K in poling field $E_p = 1.8$ V/cm.

magnetic moment of one of the hypothetic phases has to be unrealistically high.

C. Electric polarization

Electric polarization was observed only along b axis. It arises below $T_{FE} \approx 8.2$ K and increases up to 45 $\mu C/m^2$ at 2 K as shown in Fig. 5. The onset in the temperature dependence of the electric polarization corresponds to the observed anomalies in the magnetic susceptibility along b axis and perpendicular to the easy axis (α) at ≈ 8.6 K [Fig. 1(a)] as well as the onset of the incommensurate $(0.26, -\frac{1}{2}, -0.46)$ magnetic reflection (Fig. 3). Thus the observed conical spin structure can be also identified as a ferroelectric state with $\mathbf{P} \parallel b$ which is likely driven by inverse Dzyaloshinskii-Moriya magnetoelectric interaction.

At first glance the existence of the $\mathbf{P} \parallel b$ polarization makes the cycloid part of the composed (conical) phase similar to the cycloidal ferroelectric phase AF2 in pure and slightly doped (5%) MnWO$_4$.[8,15,18] However, there is a principal difference between them. In Mn$_{0.8}$Co$_{0.2}$WO$_4$ the cycloidal component of the composed spin structure is developed below T_{FE} on top of the already existing and more stable collinear AF4 phase in which spins are oriented along the easy direction in the ac plane (142° with respect to the c^* axis). So the appearance of the competing incommensurate cycloid AF2 ($\mathbf{k}_2$) spin order along the easy direction is suppressed at low temperatures and it occurs in the directions being orthogonal to the spins in the existing AF4 spin order. Thus the AF2 spin order can appear only in the magnetically hard directions. This is clearly seen from our neutron data revealing main cycloid axes along b and perpendicular to the easy direction in the ac plane (ω axis at 55° with respect to the c^* axis). This circumstance, i.e. the competition between the magnetic anisotropy and the isotropic exchange interactions stabilizing cycloid structure, could explain the observed decreasing of the ferroelectric transition temperature from ≈ 12.5 K in pure MnWO$_4$ down to ≈ 8.5 K in Mn$_{0.8}$Co$_{0.2}$WO$_4$ and likely its further suppression and disappearance with increasing Co concentration.

D. Summary and conclusions

This study of the interplay between the magnetic and ferroelectric properties in Mn$_{0.8}$Co$_{0.2}$WO$_4$ multiferroic confirms

FIG. 4. (Color online) Magnetic structures of Mn$_{0.8}$Co$_{0.2}$WO$_4$ at 11 K (a) and 2 K (b). Circles in the octahedra (green) correspond to Mn/Co, big (blue) circles between the octahedra are tungsten atoms, and smallest circles (red) are oxygen atoms. The corresponding agreement plots of the refinements are plotted on (c) and (d).

[4.6 μ_B per (Mn,Co) site in Mn$_{0.8}$Co$_{0.2}$WO$_4$ having Mn^{2+} and Co^{2+} in high-spin state].

The alternative scenario that could also result in two coexisting propagation vectors, namely the one based on phase separation with distinct volume fractions, can be ruled out since, according to the experimental intensities, the atomic
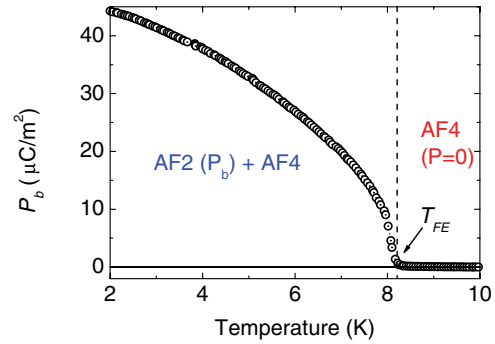
that the single-ion anisotropy of cobalt ions plays a major role in the distinct magnetic ground states of the $Mn_{1-x}Co_xWO_4$ family of magnetoelectric materials.

To summarize, we observed in $Mn_{0.8}Co_{0.2}WO_4$ by neutron diffraction, magnetic, and pyroelectric characterization measurements a coexistence of competing commensurate collinear AF4 and incommensurate cycloidal AF2 spin structures, which produces a ferroelectric ground state characterized by a conical antiferromagnetic spin order. The translational symmetry of the double-**k** magnetic structure is determined by two wave vectors $\mathbf{k}_1 = (\frac{1}{2}, 0, 0)$ and $\mathbf{k}_2 = (-0.211, \frac{1}{2}, 0.452)$. First, the collinear AF4 phase ($\mathbf{k}_1$) inherent to pure $CoWO_4$ appears at $T_N \approx 20$ K and then, decreasing temperature below $T_{FE} \approx 8.5$ K, this collinear phase coexists with the cycloidal AF2 spin structure ($\mathbf{k}_2$). This second modulation is accompanied by the appearance of ferroelectric polarization along b axis. We have found that spins in the AF4 phase are ordered along the easy direction in the ac plane, at an angle of $\approx 142°$ with respect to the c^* axis, which does not change down to the lowest temperature reached (2 K). The collinear order is clearly reminiscent of the antiferromagnetic order in $CoWO_4$ (AF4, $T_N = 55$ K, $\alpha \approx 137°$).[26] In the cycloidal AF2 structure

observed below T_{FE} the spin ordering occurs perpendicular to the easy-axis α of AF4, i.e. in magnetically hard directions that makes this structure different as compared with the pure cycloidal AF2 phase at lower cobalt concentrations. A competition between the magnetic anisotropy and isotropic exchange interactions stabilizing cycloid structure could be responsible for suppression of the ferroelectric transition temperature from ≈ 12.5 K in pure $MnWO_4$ down to ≈ 8.5 K in $Mn_{0.8}Co_{0.2}WO_4$.

*urcelay@ill.fr

[1] T. Kimura, T. Goto, H. Shintani, K. Ishizaka, T. Arima, and Y. Tokura, Nature (London) **426**, 55 (2003).

[2] D. I. Khomskii, J. Magn. Magn. Mater. **306**, 1 (2006).

[3] S.-W. Cheong and M. Mostovoy, Nat. Mater. **6**, 13 (2007).

[4] S. Ishiwata, Y. Taguchi, H. Murakawa, Y. Onose, and Y. Tokura, Science **319**, 1643 (2008).

[5] H. Katsura, N. Nagaosa, and A. V. Balatsky, Phys. Rev. Lett. **95**, 057205 (2005).

[6] I. A. Sergienko and E. Dagotto, Phys. Rev. B **73**, 094434 (2006).

[7] M. Mostovoy, Phys. Rev. Lett. **96**, 067601 (2006).

[8] G. Lautenschlager, H. Weitzel, T. Vogt, R. Hock, A. Bohm, M. Bonnet, and H. Fuess, Phys. Rev. B **48**, 6087 (1993).

[9] K. Taniguchi, N. Abe, T. Takenobu, Y. Iwasa, and T. Arima, Phys. Rev. Lett. **97**, 097203 (2006).

[10] H. Sagayama, K. Taniguchi, N. Abe, T. H. Arima, M. Soda, M. Matsuura, and K. Hirota, Phys. Rev. B **77**, 220407(R) (2008).

[11] K. Taniguchi, N. Abe, S. Ohtani, and T. Arima, Phys. Rev. Lett. **102**, 147201 (2009).

[12] F. Ye, R. S. Fishman, J. A. Fernandez-Baca, A. A. Podlesnyak, G. Ehlers, H. A. Mook, Y. Wang, B. Lorenz, and C. W. Chu, Phys. Rev. B **83**, 140401 (2011).

[13] E. García-Matres, N. Stüßer, M. Hofmann, and M. Reehuis, Eur. Phys. J. B **32**, 35 (2003).

[14] R. P. Chaudhury, B. Lorenz, Y. Q. Wang, Y. Y. Sun, and C. W. Chu, Phys. Rev. B **77**, 104406 (2008).

[15] Y.-S. Song, J.-H. Chung, J. M. S. Park, and Y.-N. Choi, Phys. Rev. B **79**, 224415 (2009).

[16] R. P. Chaudhury, B. Lorenz, Y. Q. Wang, Y. Y. Sun, and C. W. Chu, New J. Phys. **11**, 033036 (2009).

[17] L. Meddar, M. Josse, P. Deniard, C. La, G. André, F. Damay, V. Petricek, S. Jobic, M.-H. Whangbo, M. Maglione, and C. Payen, Chem. Mater. **21**, 5203 (2009).

[18] Y.-S. Song, L. Q. Yan, B. Lee, S. H. Chun, K. H. Kim, S. B. Kim, A. Nogami, T. Katsufuji, J. Schefer, and J.-H. Chung, Phys. Rev. B **82**, 214418 (2010).

[19] R. P. Chaudhury, F. Ye, J. A. Fernandez-Baca, Y.-Q. Wang, Y. Y. Sun, B. Lorenz, H. A. Mook, and C. W. Chu, Phys. Rev. B **82**, 184422 (2010).

[20] R. P. Chaudhury, F. Ye, J. A. Fernandez-Baca, B. Lorenz, Y. Q. Wang, Y. Y. Sun, H. A. Mook, and C. W. Chu, Phys. Rev. B **83**, 014401 (2011).

[21] K.-C. Liang, R. P. Chaudhury, Y. Q. Wang, Y. Y. Sun, B. Lorenz, and C. W. Chu, J. Appl. Phys. **111**, 07D903 (2012).

[22] I. Urcelay-Olabarria, E. Ressouche, A. A. Mukhin, V. Yu. Ivanov, A. M. Balbashov, G. P. Vorobev, Yu. F. Popov, A. M. Kadomtseva, J. L. García-Muńoz, and V. Skumryev, Phys. Rev. B **85**, 094436 (2012).

[23] A. M. Balbashov and S. G. Egorov, J. Cryst. Growth **51**, 498 (1981).

[24] J. Brown and J. Matthewman, Cambridge Crystallography Subroutine Library Report No. RAL93-009 (1993).

[25] J. Rodriguez-Carvajal, Physica B **192**, 55 (1993).

[26] J. B. Forsyth and C. Wilkinson, J. Phys.: Condens. Matter **6**, 3073 (1994).